

# Phase Diagram of Quasi-Two-Dimensional Carbon, From Graphene to Diamond

Alexander G. Kvashnin,<sup>†,‡,§</sup> Leonid A. Chernozatonskii,<sup>||</sup> Boris I. Yakobson,<sup>\*,†</sup> and Pavel B. Sorokin<sup>\*,‡,§,⊥</sup>

<sup>†</sup>Department of Mechanical Engineering & Materials Science and the Smalley Institute for Nanoscale Science and Technology, Rice University, Houston, Texas 77005, United States

<sup>‡</sup>Technological Institute of Superhard and Novel Carbon Materials, Moscow, 142190, Russian Federation

<sup>§</sup>Moscow Institute of Physics and Technology, Dolgoprudny, 141700, Russian Federation

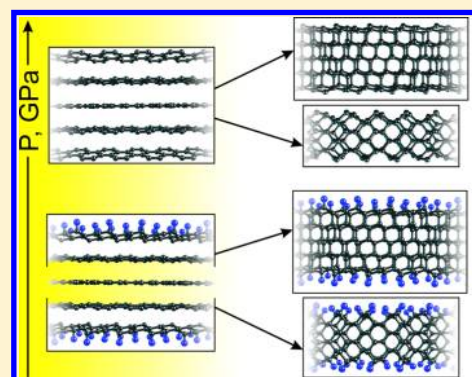
<sup>||</sup>Emanuel Institute of Biochemical Physics of RAS, Moscow, 119334, Russian Federation

<sup>⊥</sup>National University of Science and Technology MISiS, Moscow, 119049, Russian Federation

## S Supporting Information

**ABSTRACT:** We explore how a few-layer graphene can undergo phase transformation into thin diamond film under reduced or no pressure, if the process is facilitated by hydrogenation of the surfaces. Such a “chemically induced phase transition” is inherently nanoscale phenomenon, when the surface conditions directly affect thermodynamics, and the transition pressure depends greatly on film thickness. For the first time we obtain, by ab initio computations of the Gibbs free energy, a phase diagram ( $P$ ,  $T$ ,  $h$ ) of quasi-two-dimensional carbon–diamond film versus multilayered graphene. It describes accurately the role of film thickness  $h$  and shows the feasibility of creating novel quasi-two-dimensional materials. Further, the role of finite diameter of graphene flakes and possible formation of the diamond films with the (110) surface are described as well.

**KEYWORDS:** Graphene, graphane, diamane, diamond films, phase diagram, density functional theory



The discovery of new physics in graphene<sup>1–3</sup> opened a broader field of atomically thin, two-dimensional films, either obtained by graphene chemical functionalization or of different, fully noncarbon compositions. Apart from unique electronic and mechanical behaviors, the sheer openness of graphene surface (it is all surface!) makes it distinctly different from usual solids: its makeup can be entirely changed by exposure to all kinds of chemistry of hydrogenation,<sup>4,5</sup> oxidation,<sup>6</sup> fluorination,<sup>7–9</sup> or by addition of other active chemical groups to its both sides or to just one, if graphene layer was placed on a substrate. Furthermore, from few-layer graphene, nanometer thin quasi-two-dimensional diamond films can perhaps be formed, arguably as a new allotrope of carbon (once named diamane,<sup>10</sup> following similar graphene–graphane<sup>5</sup> etymology). Such films, with a surface passivated by hydrogen<sup>10</sup> or fluorine,<sup>11</sup> display the electronic structure of semiconductors, with a band gap depending on the film thickness.<sup>12</sup> The growing interest to such structures is reflected in the number of theoretical studies of the properties of thin diamond films<sup>13,14</sup> and experimental reports of multilayered graphene diamondization.<sup>15–17</sup>

The relative stability and transformation between such diamond-like and layered forms is not well understood in theory or documented from experiments. In the case of nanosized diamonds, clearly the defining role in the overall stability belongs to the surface effects which may cause the

graphitization process—the transformation of the diamond outer layers to graphene, as directly observed in diamond nanoclusters<sup>18</sup> or nanowires,<sup>19</sup> which originates from the diamond structure’s metastability. The subtle balance cannot be described by the canonical diamond–graphite phase diagram established for bulk material. The theoretical approaches of transformation of graphite to diamond which was developed previously<sup>20–24</sup> should be considerably reformulated for the application in the nanoscale case. For instance, for a single layer it was early noticed<sup>15,25,26</sup> that its full hydrogenation on both sides is thermodynamically favorable, yielding a graphane (CH), where every carbon atom is in a four-coordinated sp<sup>3</sup>-state, and consequently the overall bandgap is large as in diamonds. Such a thinnest “ultimate diamond slab”<sup>27</sup> can in principle be achieved by purely chemical means, without any pressure—in striking contrast to bulk graphite–diamond transformation which requires an enormous pressure,  $P \sim 5$  GPa. Obviously, in the latter case of bulk transformation the surface chemistry is not a significant factor, while it actually dominates the energy balance for monatomic layer. This poses a fundamental problem for quantifying this type of phase

**Received:** October 21, 2013

**Revised:** January 14, 2014

**Published:** January 17, 2014

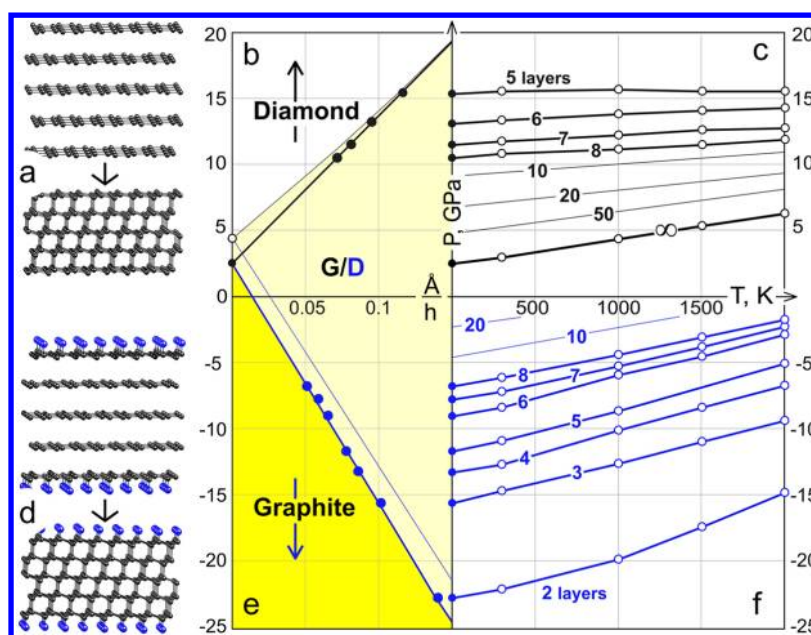


**Figure 1.** (a) Atomic structures of a five-layer graphene and the corresponding diamond film with a pristine surface. (b) The dependence of the phase transition pressure  $P$  on the inverse film thickness  $h$  at  $T = 0$  and  $1000$  K (solid and thin lines) for films with pristine surfaces. (c) The phase diagram  $P(T)$  for the  $n$ -layer graphene to a diamond film with pristine surface, for different numbers of layers (thin lines show that equilibrium curves for  $n = 10, 20$ , and  $50$  are obtained with eq 3). (d) Atomic structure of a five-layer graphene and the corresponding diamond film with hydrogenated surfaces. (e) The dependence of the phase transition pressure on the inverse film thickness  $h$  at  $T = 0$  and  $1000$  K (solid and thin lines) for films with hydrogenated surfaces. (f) The phase diagram  $P(T)$  for the transitions from a multilayer graphene to a diamond film, with a hydrogenated surface, for different numbers of layers ( $H$  is shown in blue; thin lines show the equilibrium curves for  $n = 10$  and  $20$  as obtained with eq 3).

change for the general case of  $n = 2, 3$ , or more graphene layers, when surface contribution scales as  $\sim 1/n$  (or  $\sim 1/h$  with  $h$  being the thickness of commencing diamane). Here we set forth to obtain a phase diagram that explicitly includes the effects if chemical surface hydrogenation, with the thickness  $h$  as an essential parameter, along with the usual  $P$  and  $T$ . This reveals the important conditions when the film transformation into diamond form does not require pressure at all (formally, the equilibrium line corresponds to  $P < 0$ ), or at least the usual high pressure is greatly mitigated by the surface chemistry contributions.

We begin by comparing the ab initio computed Gibbs free energies, to assess the stability of diamond films with a pristine surface and to determine the critical thickness at which a diamond would split into a stack of graphene layers. Vice versa, the obtained  $(P, T, h)$  phase diagram shows the conditions of diamond film formation from multilayered graphene. We then proceed to evaluating the formation of diamond films facilitated by chemical adsorption (of atomic H) on the multilayer graphene surface and find how the pressure of phase transition is reduced and formally turns negative, which is practically unnecessary—effectively, this becomes “chemically induced” phase transition, where both chemistry and compression concurrently serve as the driving factors for diamond film formation. We continued to study this effect through the example of the bilayer graphene flakes. It was found that as the limited surface area of graphene flake increases the pressure of the phase transition increases, while for large dimensions it asymptotically approaches the film values. Finally, we studied the atomic structures and phase diagram for both clean and hydrogenated diamond films with the (110) surface.

All calculations of the atomic and electronic structures of the diamond films were performed at a DFT (density functional

theory) level of theory in a local density approximation using the Perdew–Zunger parametrization<sup>28–30</sup> and a plane wave basis set implemented in the Quantum ESPRESSO package.<sup>31</sup> The plane-wave energy cutoff was set to 30 Ry. To calculate the equilibrium atomic structures, the Brillouin zone was sampled according to the Monkhorst–Pack<sup>32</sup> scheme with a  $8 \times 8 \times 1$   $k$ -point convergence grid. To avoid the spurious interactions between the neighboring diamond or graphite layers, the vacuum space between them was greater than 15 Å.

The phase diagram was obtained from the calculation of the Gibbs free energies  $G$  of the compared phases in the quasiharmonic approximation:<sup>33</sup>

$$G(P, T) = E_0(V) + PV + U_0(V) + F_{\text{vib}}(T, V)$$

where  $E_0$ ,  $U_0$ , and  $F_{\text{vib}}$  are the total energy from the DFT calculations, while the zero-point and vibrational energies are calculated from the following relations:

$$U_0(V) = \frac{1}{2} \int g(V, \omega) \hbar \omega \, d\omega$$

$$F_{\text{vib}}(T, V) = k_B T \int_{\Omega} g(V, \omega) \ln \left[ 1 - \exp \left( -\frac{\hbar \omega}{k_B T} \right) \right] d\omega$$

Here  $g(\omega)$  is the phonon density of states at the given pressure calculated using the density-functional perturbation theory.<sup>34</sup> The phonon density of states (PhDOS) was calculated for each value of equilibrium volume for each studied structure, using density functional perturbation theory. Then the PhDOS integrations above yield the zero-point ( $U_0$ ) and vibrational ( $F_{\text{vib}}$ ) energies, for every chosen temperature. Substitution of all the calculated energy contributions into the equation for Gibbs free energy allows one to obtain the

temperature-dependent phase transition pressure values, entered into Figure 1c and Figure 1f. The chosen approach is validated by Kern et al.<sup>33</sup> and Luo et al.<sup>35</sup> where the phase diagrams  $P(T)$  of boron nitride and carbynes were calculated, respectively, and by our calculation of the phase boundary between the diamond and graphite phases which appears close to experimental data<sup>36</sup> (see Figure S1, Supporting Information). The film volume  $V$  was evaluated as the sum of the volume per atom in the corresponding bulk states (graphite for the multilayered graphene and diamond for the diamond films).

First, the stability of the diamond films of thickness  $h = 2.48\text{--}15.67 \text{ \AA}$  (2–8 carbon layers) with pristine (111) surfaces was investigated; only the energy favorable polytypes with an ABC stacking sequence were considered. The graphitization effect leads to the transformation of the surface diamond layers into graphene. This splits the structure of the diamond film into a rhombohedral multilayered graphene when  $h = 2.48 \text{ \AA}$ . At greater thickness, the formation of a diamond core is not susceptible to surface effects. We found that the diamond films with clean surfaces became metastable when  $h > 8.42 \text{ \AA}$  ( $n > 5$  layers).

A diamond film can form by chemical bonding of the neighbor layers in a graphene stack (Figure 1a). The phase diagram of such a transition for  $T = 0\text{--}2000 \text{ K}$  is shown in the Figure 1c.

The dependence of the phase transition pressure  $P$  on the film thickness  $h$  can be analytically evaluated by incorporating the film surface energy as a small perturbation term. Our earlier study of silicon nanowires<sup>37</sup> have explicitly decomposed the energy into bulk, surface, and edge contributions, showing the importance of the surface and edge terms in determining the total energy of the structure. Similarly, here one can decompose the total film energy into its bulk and surface contributions. Moreover, since we are only concerned with the change between the two states (phases), we directly write the expression for the “deltas” of all contributions, that is, the differences between the values for one state minus another. On the thermodynamic equilibrium line such total change must be zero:

$$(\Delta G_0 + \Delta G'_0 T + P\Delta v)Sh + (\Delta\gamma_0 + \Delta\gamma'_0 T)S = 0 \quad (1)$$

Here the first part is the bulk contribution, including  $\Delta G_0$ , the difference of the Gibbs free energies per volume between bulk diamond and graphite, and the linear terms of a Taylor series of a Gibbs free energy difference at temperature  $T$  around 0 K, and in pressure  $P$ . Here  $\Delta v$  is the relative change of volume between graphene and  $sp^3$ -hybridized carbon,  $S$  is the area of a structure unit cell, and  $h$  is the film thickness. The second part of eq 1 is the surface contribution, including again  $\Delta\gamma_0$  difference of surface energies and a linear Taylor series term to correct for finite  $T > 0 \text{ K}$ .

Equation 1 can be solved for  $P$ , to yield the phase transition pressure for the films:

$$P(T, h) \cong -\frac{\Delta G_0}{\Delta v} - \frac{\Delta G'_0}{\Delta v} T - \frac{\Delta\gamma_0}{\Delta v h} - \frac{\Delta\gamma'_0}{\Delta v h} T \quad (2)$$

Relation 2 can be rewritten in the following way:

$$P(T, h) = P_0 + C_1 T + \frac{C_2 T + C_3}{h} \quad (3)$$

where  $P_0 = 2.36 \text{ GPa}$  is a pressure of bulk graphite–diamond transition at 0 K, and  $C_1$ ,  $C_2$ , and  $C_3$  are in units of  $\text{GPa/K}$ ,

$\text{GPa}\cdot\text{\AA}/\text{K}$ , and  $\text{GPa}\cdot\text{\AA}$ , respectively. The numerically obtained dependences of the phase transition pressure on the film thickness and temperature (Figure 1b–c) were fitted by the eq 3 as  $P(T, h) = 2.36 + 0.002T - (0.016T - 112.48)h^{-1}$ .

The obtained phase diagram allows us to estimate the fabrication conditions for diamond films from multilayered graphene. In a recent experimental paper<sup>16</sup> the authors reported the formation of  $sp^3$  bonds between seven-layered graphene layers at 16 GPa which agrees with our estimations that seven-layered graphene film should transit to diamond film at 12 GPa (300 K).

A large transition pressure from multilayered graphene to the diamond films makes the formation process difficult and requires the presence of a catalyst. The chemical binding with the catalyst atoms leads to a change in the chemical activity of the graphene atoms and facilitates the chemical reaction. Such an effect can be reached by the chemical binding of the surface graphene layers of a multilayered graphene film with adatoms.<sup>10,38</sup> We considered this effect using hydrogen atoms; see Figure 1d.

The phase diagram of the transition from hydrogenated multilayered graphene to hydrogenated diamond film is shown in Figure 1f. The binding of graphene with chemically adsorbed hydrogen atoms is weaker than the binding of the corresponding diamond film; therefore the transition can occur spontaneously, and the formal transition pressure is negative for this case. It means that the adsorption of adatoms to the graphene surface will lead to transformation to the  $sp^3$ -hybridized diamond film. The obtained dependence of phase transition pressure on the thickness for such process was fitted by eq 3 as  $P(T, h) = 2.36 + 0.002T - (0.012T - 139.07)h^{-1}$ . Therefore for each type of structures (clean and hydrogenated) a separate set of fitting parameters was obtained. Fitted data plotted at 0 and 1000 K (thin line) are shown in Figure 1e. The transition pressure turns to positive for the films of the thickness  $h \sim 50 \text{ \AA}$  ( $n = 25$ ) at 0 K, but its value is lower than the value of the  $P_0 = 2.36 \text{ GPa}$  of the graphite–diamond *chemically induced phase transition*. This effect is inherent to the nanoscale, where the surface contribution to thermodynamics is not negligible.

The hydrogen atom adsorption onto the multilayered graphene films surface leads to the transformation of a chemically inert  $sp^2$ -hybridized graphene lattice to a semi-hydrogenated  $sp^3$ -hybridized structure, in literature referred to as graphone.<sup>39</sup> Such layer has low stability<sup>40</sup> due to the high strain of the atomic lattice caused by the unpaired electrons of carbon atoms not bonded to the hydrogen. The binding of neighbored graphone layers forms a two-layered  $sp^3$ -hybridized diamond lattice without an activation barrier (Figure 2).<sup>14,38</sup> It is important that such a transition occurs also in the case of films with larger number of layers  $n > 2$ , approaching for  $n \gg 1$  the transformation of a rhombohedral graphite into a diamond (marked in Figure 2 by a solid black line), with a 0.4 eV/atom barrier which agrees well with published data.<sup>41,42</sup>

One may further consider the corrections to the above analysis brought about by another finite dimension, the diameter of the hydrogenated graphene flake, and how this affects its transition into the  $sp^3$ -hybridized carbon cluster. We analyzed hexagonally shaped isolated bilayer graphene flakes with AA layers stacking (Figure 3a). The chemical adsorption of the hydrogen atoms to the alternating carbon atoms of both layers leads to the corrugation of the layer with displacement of the neighboring atom in the plane due to  $sp^3$  hybridization.

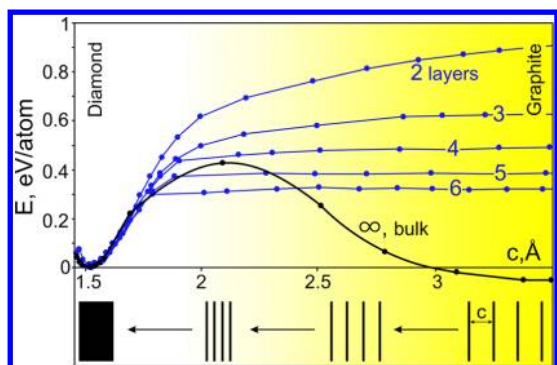


**Figure 2.** Potential energy curves showing the transition from rhombohedral multilayer graphene with hydrogenated surface, with different thicknesses ( $n = 2-6, \infty$ ) into diamond films (chosen as zero energy level). The transition of the bulk rhombohedral graphite to diamond is shown by a bold black line. All energies are plotted versus the average distance  $c$  between the neighbor layers. The schematics at the bottom illustrate the transition.

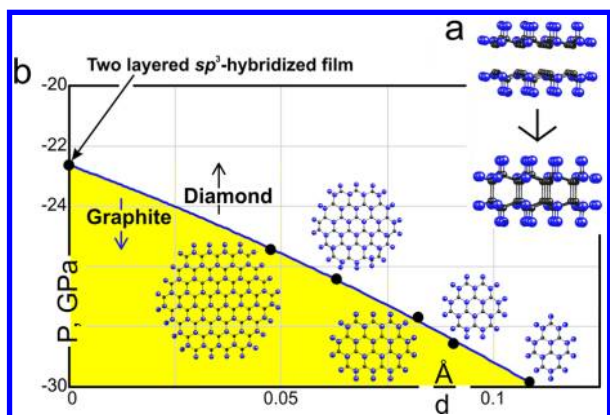


**Figure 3.** (a) Structures of hydrogenated bilayer graphene flakes and corresponding  $sp^3$ -hybridized clusters. (b) Dependence of the phase transition pressure on the size  $d$  of bilayer flakes, at 0 K.

Such atoms tend to bind with the neighboring graphene flake and form a diamond cluster. In this case, the phase transition pressure depends both on the thickness  $h$  and diameter  $d$  of the graphene flake ( $sp^3$ -hybridized cluster), in approximation of a

circular-disk shape (see Supporting Information for details). The phase transition pressure in this case appears in the form:

$$P(T = 0) = P_0 + \frac{A}{h} + \frac{B}{dh} + \frac{C}{d^2} \quad (4)$$

where  $P_0$  is a graphite-diamond phase transition pressure,  $h$  is the thickness in angstroms, and  $d$  is the size (diameter) of a flake ( $sp^3$  hybridized film).

In the limiting case of a structure with an infinitely large area ( $d \rightarrow \infty$ ), the expression (4) tends to eq 3 at 0 K for laterally infinite films (see Supporting Information for details).

The feasibility of the obtained relationship is illustrated by the calculations of pressure of transition between hydrogenated bilayered graphene flake and the corresponding  $sp^3$ -hybridized cluster (Figure 3b). The dependence of the phase transition pressure on the flake size was fitted by the eq 4 as  $P(T = 0, h = 2.48 \text{ \AA}) = -22.64 - 51.9d^{-1} - 135.8d^{-2}$ , where the pressure of  $-22.64 \text{ GPa}$  is the phase transition pressure of a two-layered film. It should be noted that for large graphene flakes only the first term is sufficient; therefore the transition pressure is proportional to  $d^{-1}$ .

The organization of adatoms (which may depend on adatom type and external conditions) on the graphene surface is critical in this issue. It is known that besides the chair<sup>1</sup><sup>43</sup> (usually referred to simply as “chair”) conformation, graphene has a low energy chair<sup>2</sup><sup>43</sup> (“washboard”,<sup>44</sup> “stirrup”<sup>45</sup>) configuration which also can be considered as the first member of the diamond film family with the (110) surface. Therefore the adsorption of the adatoms to the surface of the multilayered graphene in chair2 configuration will lead to the formation of the diamond film with the (110) surface.

Let us consider diamond films with a (110) surface. Instead of previously studied films, such structures consist of only one polytype at any thickness. For example, in Figure 4a the atomic structures of single layered diamond film with a (110) surface (graphane of a chair2 conformation) and five layered diamond films with a hydrogenated and clean (110) surface are presented. Another important issue is that the films with only odd indexes can be decomposed to the isolated single layers; therefore, only half of the structures can be obtained by using multilayered graphene as a precursor, whereas the other part should be synthesized by other methods (e.g., using CVD growth).

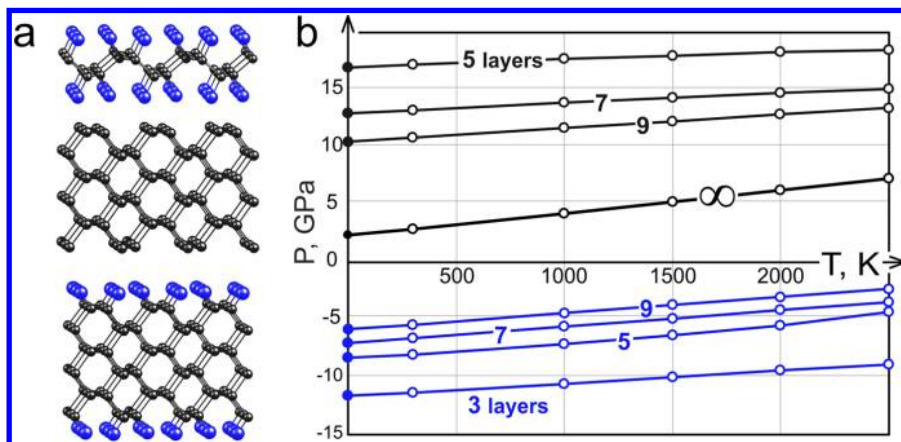


**Figure 4.** (a) Atomic structure of chair2 conformation graphane (top) and five-layer diamond films with pristine (middle) and hydrogenated (bottom) (110) surfaces. (b) The phase diagram for diamond films with a (110) surface. For the cases of pristine or hydrogenated surfaces, the corresponding curves are black or blue.

Like in the case of the (111) oriented films in such diamond nanostructures, the surface effect also plays a major role in the stability and atomic structure (the electronic properties are discussed in the Supporting Information). Due to the graphitization effect, unpassivated films only with a thickness larger than 5.75 Å (five carbon layers) are stable. The thinnest film can be formed at the pressure 16.9 GPa by the connection of three graphene layers.

The chemically induced phase transition for the diamond films occurs in a similar manner like as the (111) diamond films (Figure 4b). Hydrogenation leads to a negative phase transition pressure for diamond films with a (110) hydrogenated surface due to a change in the reactivity of the hydrogenated outer layers of the multilayered graphene films, which indicates the possibility of the chemically induced phase transition realization in these cases as well.

As mentioned above, the realization of the proposed chemically induced phase transition depends on a number of factors. In support of its feasibility, one should note the experimental papers<sup>15,17</sup> reporting the formation of interlayer bonds in multilayered graphene caused by the attachment to the surface of hydroxyl groups and hydrogen, respectively. Although the graphene in ref 17 is supported by platinum substrate, the principle mechanism of phase transition is the same as described here, with one minor difference: whereas the upper graphene layer changes the hybridization due to the adsorption of hydrogen atoms, the bottom layer binds covalently to the platinum atoms. Further, our results are closely related with the papers<sup>46,47</sup> reporting the diamondization of graphite and amorphous carbon, caused by attaching fluorine and hydrogen, respectively. Note that, according to ref 46, the fluorination of graphite leads to the formation of  $sp^3$ -hybridized  $C_2F$  films. In the next report from the same group, the X-ray, NMR, and electronic microscopy analyses<sup>48</sup> show that fluorinated graphite of  $C_2F$  stoichiometry is a stack of ordered thinnest two-layered diamond films.

The phase diagram of the carbon films of nanometer thickness (multilayered graphene and diamond films) was obtained using ab initio calculation methods. The phase transition was studied for films with both passivated and clean surfaces and of different crystallographic orientations. The diamond films with (110) surface were considered for the first time. The phase diagram for both hydrogenated and clean diamond films with (110) surface was carefully mapped out. It was found that chemically induced phase transition should occur in a similar manner as for the (111) diamond films. The effect of “chemically induced phase transition” was studied in detail, yet only from thermodynamics standpoint. One should keep in mind that the actual transition and especially its rate must depend greatly on the (new phase) nucleation process, its “reaction path”, and nucleation barrier. These aspects are far beyond the scope of our present report. Nevertheless, the obtained agreement with experimental data<sup>16</sup> supports using similar approach to construct phase diagrams for different carbon (and other) materials nanostructures where the small dimensions permit surface chemistry to affect the overall thermodynamics balance.

## ■ ASSOCIATED CONTENT

### Supporting Information

Information about the calculation of diamond/graphite and graphene flake/diamond cluster phase boundaries; data of evolution of the electronic structure of the (110) diamond films

with nanometer thickness. This material is available free of charge via the Internet at <http://pubs.acs.org>.

## ■ AUTHOR INFORMATION

### Corresponding Authors

\*E-mail: [biy@rice.edu](mailto:biy@rice.edu).

\*E-mail: [pbsorokin@gmail.com](mailto:pbsorokin@gmail.com).

### Notes

The authors declare no competing financial interest.

## ■ ACKNOWLEDGMENTS

We are grateful to the Moscow State University for use of the cluster computers “Chebishev” and “Lomonosov”. This work was supported by the Ministry of Education and Science of the Russian Federation (contracts no. 14.B37.21.1645 and no. 11.G34.31.0061) and the Russian Foundation for Basic Research (project no. 12-02-31261). A.G.K. acknowledges the Scholarship of President of Russia for Young Scientists and Ph.D. Students (competition SP-2013). L.A.C. acknowledges the Russian Foundation for Basic Research (project no. 11-02-01453-a) and “FAEMCAR” (FP7-PEOPLE-2012-IRSES). Work at Rice was supported by the US Air Force Office of Scientific Research grant FA9550-12-1-0035 (MURI) and by the Office of Naval Research MURI grant N00014-09-1-1066.

## ■ REFERENCES

- (1) Novoselov, K. S.; Jiang, D.; Schedin, F.; Booth, T. J.; Khotkevich, V. V.; Morozov, S. V.; Geim, A. K. *Proc. Natl. Acad. Sci. U.S.A.* **2005**, *102* (30), 10451–10453.
- (2) Neto, A. H. C.; Guinea, F.; Peres, N. M. R.; Novoselov, K. S.; Geim, A. K. *Rev. Mod. Phys.* **2009**, *81*, 109–162.
- (3) Terrones, M.; Botello-Méndez, A. R.; Campos-Delgado, J.; López-Urías, F.; Vega-Cantú, Y. I.; Rodríguez-Macías, F. J.; Elías, A. L.; Muñoz-Sandoval, E.; Cano-Márquez, A. G.; Charlier, J. C.; et al. *Nano Today* **2010**, *5* (4), 351–372.
- (4) Elías, D. C.; Nair, R. R.; Mohiuddin, T. M. G.; Morozov, S. V.; Blake, P.; Halsall, M. P.; Ferrari, A. C.; Boukhvalov, D. W.; Katsnelson, M. I.; Geim, A. K.; et al. *Science* **2009**, *323*, 610–613.
- (5) Sofo, J. O.; Chaudhari, A. S.; Barber, G. D. *Phys. Rev. B* **2007**, *75* (15), 153401.
- (6) Mathkar, A.; Tozier, D.; Cox, P.; Ong, P.; Galande, C.; Balakrishnan, K.; Reddy, A. L. M.; Ajayan, P. M. *J. Phys. Chem. Lett.* **2012**, *3* (8), 986–991.
- (7) Nair, R. R.; Ren, W.; Jalil, R.; Riaz, I.; Kravets, V. G.; Britnell, L.; Blake, P.; Schedin, F.; Mayorov, A. S.; Yuan, S.; et al. *Small* **2010**, *6* (24), 2877–2884.
- (8) Robinson, J. T.; Burgess, J. S.; Junkermeier, C. E.; Badescu, S. C.; Reinecke, T. L.; Perkins, F. K.; Zalalutdinov, M. K.; Baldwin, J. W.; Culbertson, J. C.; Sheehan, P. E.; et al. *Nano Lett.* **2010**, *10* (8), 3001–3005.
- (9) Zbořil, R.; Karlický, F.; Bourlinos, A. B.; Steriotis, T. A.; Stubos, A. K.; Georgakilas, V.; Šafářová, K.; Jančík, D.; Trapalis, C.; Otyepka, M.; et al. *Small* **2010**, *6* (24), 2885–2891.
- (10) Chernozatonskii, L. A.; Sorokin, P. B.; Kvashnin, A. G.; Kvashnin, D. G. *JETP Lett.* **2009**, *90* (2), 134–138.
- (11) Ribas, M. A.; Singh, A. K.; Sorokin, P. B.; Yakobson, B. I. *Nano Res.* **2011**, *4* (1), 143–152.
- (12) Chernozatonskii, L. A.; Sorokin, P. B.; Kuzubov, A. A.; Sorokin, B. P.; Kvashnin, A. G.; Kvashnin, D. G.; Avramov, P. V.; Yakobson, B. I. *J. Phys. Chem. C* **2011**, *115* (1), 132–136.
- (13) Leenaerts, O.; Partoens, B.; Peeters, F. M. *Phys. Rev. B* **2009**, *80* (24), 245422.
- (14) Yuan, L.; Li, Z.; Yang, J.; Hou, J. G. *Phys. Chem. Chem. Phys.* **2012**, *14* (22), 8179–8184.
- (15) Barboza, A. P. M.; Guimaraes, M. H. D.; Massote, D. V. P.; Campos, L. C.; Neto, N. M. B.; Cancado, L. G.; Lacerda, R. G.;

Chacham, H.; Mazzoni, M. S. C.; Neves, B. R. A.; et al. *Adv. Mater.* **2011**, *23* (27), 3014–3017.

(16) Clark, S.; Jeon, K. J.; Chen, J. Y.; Yoo, C. S. *Solid State Commun.* **2013**, *154*, 15–18.

(17) Rajasekaran, S.; Abild-Pedersen, F.; Ogasawara, H.; Nilsson, A.; Kaya, S. *Phys. Rev. Lett.* **2013**, *111* (8), 085503.

(18) Kuznetsov, V. L.; Butenko, Y. V. *Synth., Prop. Applications Ultrananocrystalline Diamond* **2005**, *192*, 199–216.

(19) Shang, N.; Papakonstantinou, P.; Wang, P.; Zakharov, A.; Palnitkar, U.; Lin, I. N.; Chu, M.; Stamboulis, A. *ACS Nano* **2009**, *3* (4), 1032–1038.

(20) Sung, J. *J. Mater. Sci.* **2000**, *35* (23), 6041–6054.

(21) Tian, F.; Dong, X.; Zhao, Z.; He, J.; Wang, H. T. *J. Phys.: Condens. Matter* **2012**, *24*, 165504.

(22) Dong, X.; Zhou, X. F.; Qian, G. R.; Zhao, Z.; Tian, Y.; Wang, H. T. *J. Phys.: Condens. Matter* **2013**, *25*, 145402.

(23) Tateyama, Y.; Ogitsu, T.; Kusakabe, K.; Tsuneyuki, S. *Phys. Rev. B* **1996**, *54* (21), 14994–15001.

(24) Wang, J. T.; Chen, C.; Kawazoe, Y. *Phys. Rev. B* **2011**, *84* (1), 012102.

(25) Sluiter, M. H. F.; Kawazoe, Y. *Phys. Rev. B* **2003**, *68* (8), 085410.

(26) Lin, Y.; Ding, F.; Yakobson, B. I. *Phys. Rev. B* **2008**, *78* (4), 041402(R).

(27) Muñoz, E.; Singh, A. K.; Ribas, M. A.; Penev, E. S.; Yakobson, B. I. *Diam. Relat. Mater.* **2010**, *19* (5–6), 368–373.

(28) Hohenberg, P.; Kohn, W. *Phys. Rev.* **1964**, *136* (3B), B864–B871.

(29) Kohn, W.; Sham, L. J. *Phys. Rev.* **1965**, *140* (4), A1133–A1138.

(30) Perdew, J. P.; Zunger, A. *Phys. Rev. B* **1981**, *23* (10), 5048–5079.

(31) Giannozzi, P.; Baroni, S.; Bonini, N.; Calandra, M.; Car, R.; Cavazzoni, C.; Ceresoli, D.; Chiarotti, G. L.; Cococcioni, M.; Dabo, I.; et al. *J. Phys.: Condens. Matter* **2009**, *21*, 395502.

(32) Monkhorst, H. J.; Pack, J. D. *Phys. Rev. B* **1976**, *13* (12), 5188–5192.

(33) Kern, G.; Kresse, G.; Hafner, J. *Phys. Rev. B* **1999**, *59* (13), 8551–8559.

(34) Baroni, S.; de Gironcoli, S.; Dal Corso, A.; Giannozzi, P. *Rev. Mod. Phys.* **2001**, *73* (2), 515–562.

(35) Luo, W.; Windl, W. *Carbon* **2009**, *47* (2), 367–383.

(36) Bundy, F. P. *Physica A* **1989**, *156* (1), 169–178.

(37) Zhao, Y.; Yakobson, B. I. *Phys. Rev. Lett.* **2003**, *91* (3), 035501.

(38) Zhu, L.; Hu, H.; Chen, Q.; Wang, S.; Wang, J.; Ding, F. *Nanotechnology* **2011**, *22* (18), 185202.

(39) Zhou, J.; Wang, Q.; Sun, Q.; Chen, X. S.; Kawazoe, Y.; Jena, P. *Nano Lett.* **2009**, *9* (11), 3867–3870.

(40) Podlivaev, A. I.; Openov, L. A. *Semiconductors* **2011**, *45* (7), 958–961.

(41) Fahy, S.; Louie, S. G.; Cohen, M. L. *Phys. Rev. B* **1986**, *34* (2), 1191–1199.

(42) Furthmüller, J.; Hafner, J.; Kresse, G. *Phys. Rev. B* **1994**, *50* (21), 15606–15622.

(43) Wen, X. D.; Hand, L.; Labet, V.; Yang, T.; Hoffmann, R.; Ashcroft, N. W.; Oganov, A. R.; Lyakhov, A. O. *Proc. Natl. Acad. Sci. U.S.A.* **2011**, *108* (17), 6833–6837.

(44) Artyukhov, V. I.; Chernozatonskii, L. A. *J. Phys. Chem. A* **2010**, *114* (16), 5389–5396.

(45) Bhattacharya, A.; Bhattacharya, S.; Majumder, C.; Das, G. P. *Phys. Rev. B* **2011**, *83* (3), 033404.

(46) Watanabe, N. *Solid State Ionics* **1980**, *1* (1–2), 87–110.

(47) Lifshitz, Y.; Kohler, T.; Frauenheim, T.; Guzman, I.; Hoffman, A.; Zhang, R. Q.; Zhou, X. T.; Lee, S. T. *Science* **2002**, *297* (5586), 1531–1533.

(48) Touhara, H.; Kadono, K.; Fujii, Y.; Watanabe, N. *Z. Anorg. Allg. Chem.* **1987**, *544* (1), 7–20.

(49) N'Diaye, A. T.; Bleikamp, S.; Feibelman, P. J.; Michely, T. *Phys. Rev. Lett.* **2006**, *97* (21), 215501.

(50) Odkhuu, D.; Shin, D.; Ruoff, R. S.; Park, N. *Scientific Reports* **2013**, *3*, 3276.

## ■ NOTE ADDED IN PROOF

We note that similar chemically induced phase transition can be more feasible practically in an asymmetric configuration, when graphene "reacts" with metal substrate on the one side<sup>49</sup> while is exposed to an active H or F on the other, as discussed in a very recent report.<sup>50</sup>